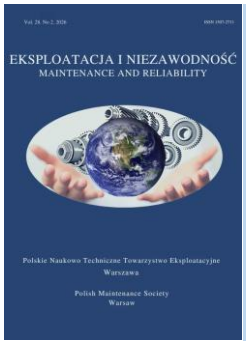

Eksploatacja i Niezawodnosc – Maintenance and Reliability
Volume 28 (2026), Issue 2
journal homepage: http://www.ein.org.pl

Article citation info:
Ismail Baran M, Aytaç Onur Y, Experimental, theoretical and numerical investigations on the monitoring of reliability of elevator guide rail bracket under safety device activated, Eksploatacja i Niezawodnosc – Maintenance and Reliability 2026: 28(2) http:/10.17531/ein/211208

Experimental, theoretical and numerical investigations on the monitoring of reliability of elevator guide rail bracket under safety device activated

Indexed by:
Web of Science Group

Muhammet Ismail Baran[a], Yusuf Aytaç Onur[a,*]

[a] Mechanical Engineering, Zonguldak Bulent Ecevit University, Turkey

Highlights

- Experimental instrumentation have been conducted on the elevator guide rail bracket.
- Elevator investigated was subjected to a full load braking test.
- Normal stress variation during braking process were measured by using strain gages.
- The most critical loading type is found as loading of three fourth of cabin at front.
- The maximum equivalent stress increased by 8.44% when the cabin was loaded at front compared to right-side loading .

Abstract

The rapidly increasing world population, high urbanization rates of countries and shrinking living spaces have forced people to live in multi-storey buildings. Guide rails and guide rail brackets are used to connect guide rails to the wall of elevator shaft. In this study, behaviour of guide rail and rail brackets against free fall of a passenger elevator is investigated by taking into account different loading and operating combinations considering related standards. Elevator guide rail and its bracket are computer aided modelled and finite element analyses are performed. In addition, experimental instrumentation and measurements have been conducted on the elevator guide rail bracket so that emergency braking reliability of elevator guide rail components can be evaluated when the elevator is loaded with 125% of its maximum capacity and the cabin goes into free fall due to reasons such as rope breakage. It can be concluded from the findings that dynamic effects during the running and braking of the elevator have an effect of 20% compared to the results of the static analysis.

Keywords
experimental instrumentation, reliability monitoring, finite element analysis, elevator guide rail brackets

This is an open access article under the CC BY license (https://creativecommons.org/licenses/by/4.0/)

1. Introduction

Elevator is defined as a conveyance designed to transport people or freights vertically. Elevator is used to satisfy the traffic demands between floors in multi-storey buildings [1]. The continuous increase in the urbanization and high-rise buildings promoted the rate of daily elevator use in human life. The fact that the human factor is in the theme of the subject makes safety and comfortable travel issues of elevators inevitable. Elevators have many sub-parts which help its vertical movement and stopping [2]. The main elements that contribute to the safe operation of elevators are the wire ropes or belts, car frame, guide rail and its bracket system and safety gear respectively. For a proper, comfortable, and safe travel guide rail and its bracket are critical components in elevator system [3]. Earthquake disasters have shown that installed facilities in buildings such as elevators must include security precautions. Guide rails and guide rail brackets connecting guide rails to the walls of elevator shaft are critical for safe travel of elevators. Guide rails provide vertical movement of elevator and prevent lateral movement and those work together with the guide shoes and safety gear which are important parts for the safe operation of the elevator installations [4,5]. The safety gear is designed to stop the elevator car or counterweight by clamping onto the

(*) Corresponding author.
E-mail addresses: I. Baran, ytcnr@yahoo.com, Y. Onur (ORCID: 0000-0002-4122-0486) aytaconur@hotmail.com

guide rails if the car's speed exceeds a predetermined limit during downward travel [6,7]. It is typically installed on the bottom channels of the car frame and is triggered by the governor rope [8]. Theoretical and numerical calculations of elevator guide rails, behaviour of clips and bolts that are used to guide rail anchor and stress distribution on the elevator guide rail at different elevator car positions using finite element(FE) method have been investigated [9-11]. Effects of noncompliant braking distances, mechanical models of elevator guide shoes and parameters of geometric displacement of guide rails have been measured [12-14]. Previous studies generally focused on FE modeling and analysis of elevator parts including guide rail and bracket rather than experimental studies since it is very difficult to carry out elevator experimental tests due to reasons such as obtaining permission to participate in full load tests during the elevator licensing process and the lack of mounting space yields hassle of connecting sensor in the elevator shaft. Zhang et al. [15] investigated dynamic performance of a monorail crane under different braking parameters to evaluate the emergency braking reliability. Effects of traction speed, load and friction coefficient on fatigue life of elevator drum brakes under emergency braking and effect of mechanism of a three-sided arc fairing on pressure distribution surrounding airflow velocity, and aerodynamic drag of elevator cars have been investigated [16-17]. Niu et al. [18] establishes an elevator performance evaluation index system by fully analyzing the elevator operation mechanism. It was expected that the proposed system could be applied to the actual evaluation and maintenance system to play a positive role in condition monitoring of elevators. Lee et al. [19] performs an experimental study that uses a full-scale mock-up to evaluate the effects of pressure differences on the functioning of elevator doors. Zhang et al. [20] studies a horizontal vibration suppression strategy for a high-speed elevator car frame system based on explicit model predictive control. In this study, a gearless passenger elevator that has already been installed in a building located in Zonguldak-Turkey province was examined. It consists of 7 stops with nominal load of 800 kg. TS EN 81-50 and TS EN 81-20 standards [21,22] are considered in the analytical calculations. Mechanical stresses, deflections and forces exerted upon guide rail and its bracket taking into account different operating and loading combinations of investigated passenger elevator have been determined where the safety gear is activated. Elevator guide rail and its bracket are computer aided modeled. The forces obtained as a result of the analytical analysis were applied to the guide rail and finite element analyses have been performed. In addition, experimental instrumentation and measurements have been conducted on the elevator guide rail bracket so as to attain experimental findings which are rather difficult to perform and measure. While stresses on an elevator rail bracket with a carrying capacity of 2000 kg were analyzed numerically under static loads in [23] and static shear tests of bolt and clip of guide rail bracket outside the real elevator installation were conducted in [10], in addition to the literature, in the study, the stresses on the guide rail bracket were determined experimentally through in-situ free fall tests performed when the nominal load was increased by 125% and loaded homogeneously in the elevator car. This work fills a gap in the current literature of experimental studies carried out on elevator guide rail and its bracket since there is not any study in the literature on experimental instrumentation and measurement of elevator guide rail components in the elevator shaft.

2. Guide rail connection system

In elevators, guide rails, brackets and nails constitute the guide rail connection system. Guide rail connection system connects guide rails to the walls of elevator shaft which is critical issue for safe travel of elevators. Their functions in the elevator system can be listed as providing connections between components, safety, aligning the rails for a comfortable journey, fixing them to prevent vibrations, providing flexibility in joining the rails at a certain angle, and providing ease of disassembly in case of possible maintenance. Figure 1 shows guide rail connection system.

Guide rails are manufactured by two different methods after the rolling process. The first of these is cold drawing which is the common production method and the second is the machining method. Those are manufactured in certain length. In cases where the required level difference is greater than raw height, the rails are assembled by adding them to each other.

After the two guide rails are aligned, connection plates including bolt holes are used to make guide rails line up vertical direction. Guide rail brackets serve to attach the elevator car and

counterweight rails securely to the building and it restrains lateral displacement of the rails through nails, and absorb loads that occur during operation or during an earthquake.

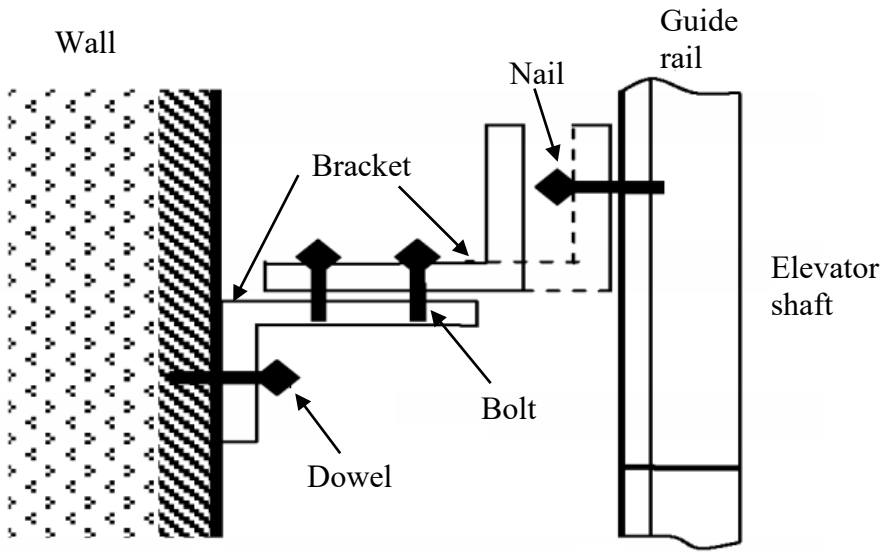

Fig. 1. Typical guide rail connection system.

The most dangerous situation that may be encountered under seismic loads is the collision of the cabin and the counterweight due to deformation in the brackets that results in coming off the rails. The bracket system is selected considering status of the project, carried load parameters and earthquake risk of the region. The connection of the guide rail brackets to the well concrete is made by means of steel dowels. While the construction phase continues, the well wall applies pressure to the guide rails via brackets. These forces cause damage to the guide rails over time. This is basically the reason why rail nail is used [23].

2.1. Methodology of analytical calculation of guide rail connection system

In this study, a gearless passenger elevator that has already been installed in a building located in Zonguldak-Turkey province was examined. It consists of 7 stops with nominal load of 800 kg. TS EN 81-50 and TS EN 81-20 standards are considered in the analytical calculations. When the safety device is activated and the elevator car moves in the vertical direction, it creates forces along the *x, y* and *z* axes of the guide rail through its shoes. Those forces yield bending stress, rail neck (flange) bending, buckling stress, combined stresses and deflection on the guide rail [24]. This study examines a T 89/B type guide rail and an elevator cabin guided with a 70 mm offset from the center. Figure 2 shows the exact dimensions of the eccentrically guided elevator car used in the study.

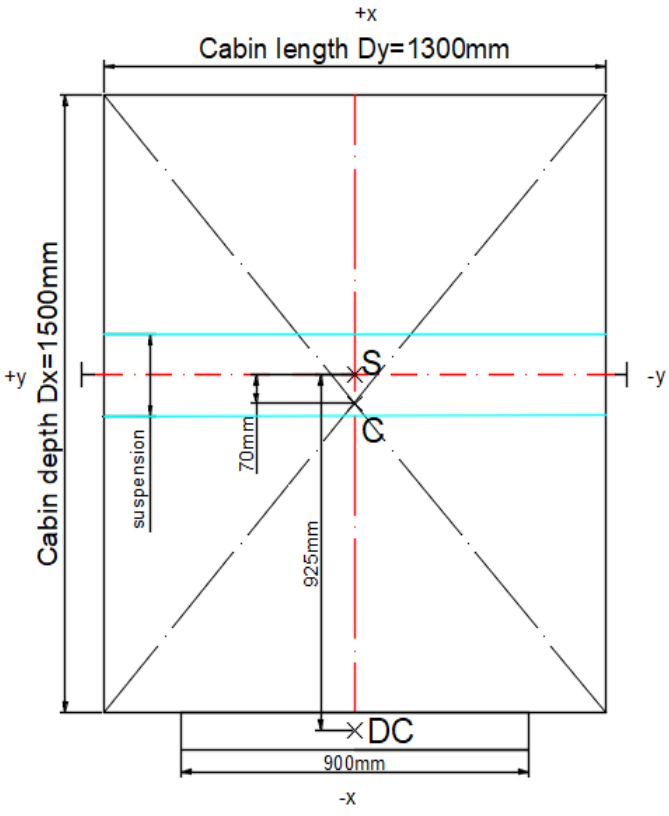

Fig. 2. Dimensions of the eccentrically guided elevator car investigated.

C is the geometric center of elevator cabin, *S* is suspension point and *DC* is the door center in Figure 2. Design and calculation parameters are given in Table 1.

Table 1. Parameters for calculations.

Guide rail	**T89/B (89x62x16mm)**	**Total cabin weight**	**P=800kg**
Suspension weight	F_{Fr} =200kg	**Rated load**	Q=800kg
Empty cabin weight	F_c=400kg	**Length between shoes**	h=3200mm
Door weight	F_{D1}=100kg	**Length between brackets**	l=2500mm
Other part weights	F_a=100kg	**Number of guide rail**	n=2

In the study, analytical calculations were made separately for the cases that load distribution is located at the right (Figure 3b), front (Figure 3a) and homogeneous load distributions (Figure 3c) within the cabin. Drawings of those conditions are given in Fig. 3.

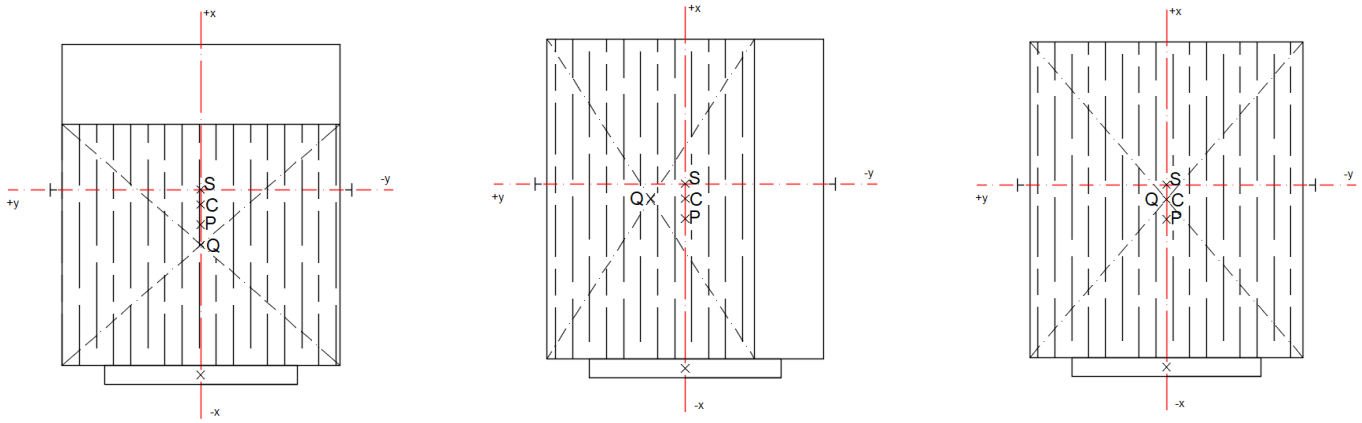

(a) (b) (c)

Fig. 3. Different load combinations of the loads in the cabin.

In Figure 3, *P* is centroid of empty cabin, Q is centroid of nominal load.

According to related standards, cabin load distribution is made in analytical calculations for the worst cases where load distribution is considered to be at the front and right and distributed equally to ¾ of the cabin as depicted in Figure 3a and 3b. In addition to this calculation, as a contribution to the literature, the calculations were repeated by creating a third loading condition in which the load distribution was homogeneous throughout the cabin as depicted in Figure 3c and the declared load was increased by 125% to enable comparison with experimental results. Bending stress must be taken into account when sizing guide rails. In cases where the safety device acts on the rail, both bending and buckling stresses, which are the vertical direction caused by the weight of the cabin, should be taken into account [25]. Machined guide rail and forces acting on the elevator guide rail in the standard are depicted in Figure 4.

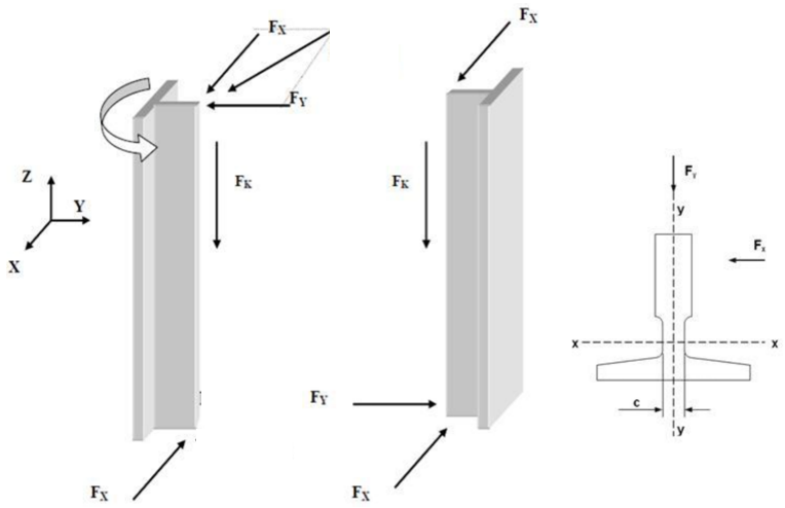

Fig. 4. Section view and axial forces acting on guide rail.

Cross sectional dimensions of investigated T89/B type guide rail are shown in Table 2.

Table 2. Cross sectional dimensions of investigated T89/B type guide rail.

Short symbol	b	h	k	n	c	f	g
T89/B	89	62	16	34	10	11.1	7.9

The F_x and F_y given in Figure 4b are found by using equation 1 and 2 respectively. Figure 3 and Figure 4 are used together to obtain the bending moments (in x and y directions) about the suspension point of the elevator cabin and those moment calculations help to find F_x and F_y forces.

$$F_x = \frac{k_1.g_n.(Q.x_Q+P.x_P)}{n.h}; M_y = \frac{3.F_x.l}{16}; \sigma_y = \frac{M_y}{W_y} \quad (1)$$

$$F_y = \frac{k_1.g_n.(Q.y_Q+P.y_P)}{\frac{n}{2}.h}; M_x = \frac{3.F_y.l}{16}; \sigma_x = \frac{M_x}{W_x} \quad (2)$$

The bending moment (M_y) and bending stress (σ_y) in the guide rail is found using equation 1. The bending moment (M_x) and bending stress (σ_x) in the guide rail due to forces in the x-axis is found using equation 2. Buckling force and stress are found by using equation 3.

$$F_k = \frac{k_1.g_n.(P+Q)}{n};\ \sigma_k = \frac{(F_k+k_3.M)}{A}.\omega \quad (3)$$

Bending and compression cause combined stress on the guide rail and it is formulated as equation 4.

$$\sigma = \sigma_x + \sigma_y + \frac{F_k+k_3.M}{A} \leq \sigma_{zul} \quad (4)$$

Equation 5 shows bending stress occurred on the guide rail neck.

$$\sigma_F = \frac{(1.85).F_x}{c^2} \leq \sigma_{zul} \quad (5)$$

Equation 6 and equation 7 show guide rail bending (deflection) values in the x and y axes.

$$\delta_y = (0.7).\frac{F_y.l^3}{48.E.I_x} \quad (6)$$

$$\delta_x = (0.7).\frac{F_x.l^3}{48.E.I_y} \quad (7)$$

where k_1 and k_3 are impact coefficients corresponding to braking type, g_n is gravitational acceleration (m/s^2), x_Q and y_Q are distance between centroid of nominal load (full cabin) and origin (mm) that are calculated taking into account load distribution status in Figure 3, x_P and y_P are distance between cabin (empty) centroid and origin (mm) that are calculated taking into account load distribution status in Figure 3, W_x and W_y are section modulus (mm^3), M is force due to auxiliary equipment (N), ω is omega value due to buckling, A is guide rail cross-sectional area (mm^2), σ_{zul} is endurance stress (MPa), c is guide rail neck width (mm), I_x and I_y represent the moments of inertia around the x- and y-axes (mm^4), E is Young's modulus (MPa).

In the front loading case, $x_Q = \frac{D_x}{8} - x_C = \frac{1500mm}{8} - (-70) = 257.5mm$ and $y_Q = 0$ are determined by using Figure 3a and the definition above. In the right loading case, $x_Q = x_C = -70mm$ and $y_Q = \frac{D_y}{8} = \frac{1300mm}{8} = 162.5mm$ are determined by using Figure 3b and the definition above. In the homogeneous loading case $x_Q = x_C = -70mm$ and $y_Q = 0$ are determined by using Figure 3c and the definition above.

2.2. Simulation studies of the guide rail connection system

3D solid models of the T 89/B guide rail, seventh console system from the bottom of the well and connecting nails have been designed in the SolidWorks. While designing these components, dimensions taken from the installation company have been used. Individual and full system drawings of the components of the system of guide rail connection are depicted in Figure 5 and Figure 6 respectively and material properties are given in Table 3.

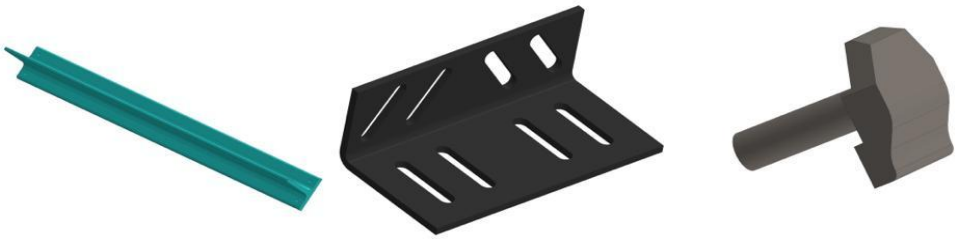

Fig. 5. SolidWorks drawings of system components.

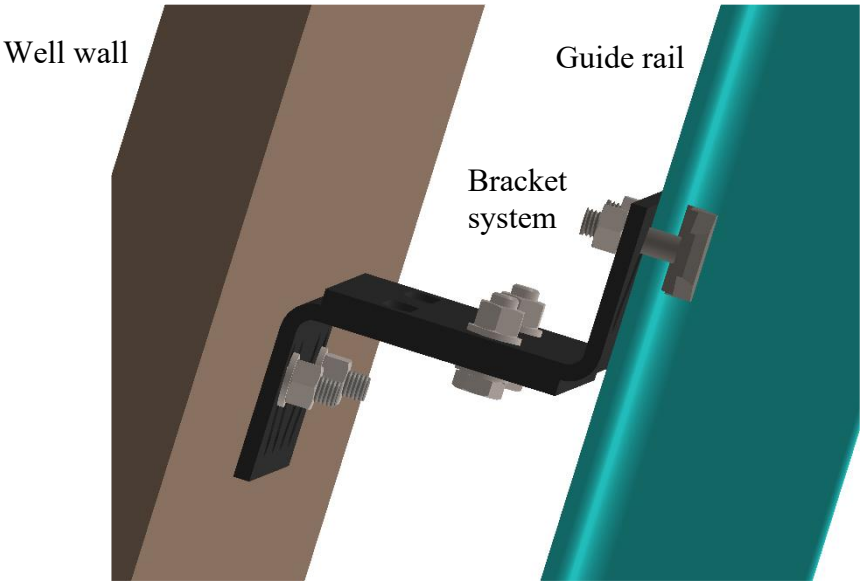

Fig. 6. 3D model of the guide rail mounted on the well wall.

Table 3. Material properties.

	Material	Density (kg/m^3)	Young modulus (E)(GPa)	Poisson's ratio	Yield strength (MPa)
Guide rail	St 37	7800	210	0.28	235
Connection nail	Cm 45	7850	205	0.29	530
Rail bracket	St 42	7800	210	0.28	275

Finite element method (FEM) was used for numerical analysis of the system. It is a numerical analysis method that is highly preferred in engineering and science fields such as structural analysis. With this method, structures with complex geometry are divided into simple elements such as rectangles and triangles. Each element represents mathematical equations and physical parameters. FEM is used to analyse the physical effects of stresses and deformations in structural elements [26]. Elevator guide rail connection system (EGCS) including nails, rail, washers, nuts, steel dowels and bolts have been assembled in SolidWorks.

The mechanical model of EGCS was exported to Ansys Workbench and the static structural section of the software was selected to analyse the behavior of system. Then, the structural steel material was selected and the properties in Table 3 were defined in the software. The assembly consists of multiple parts and these solid parts are in motion with each other. Frictional contact type was defined for the upper bracket-rail contact and bonded contact type is defined for the lower bracket-upper bracket and lower bracket-dowel contact.

Hexadron(bricks) element was used in the meshing process of EGCS. The model is divided into 24647 elements and 118703 nodes. Figure 7 shows meshed finite element model of EGCS.

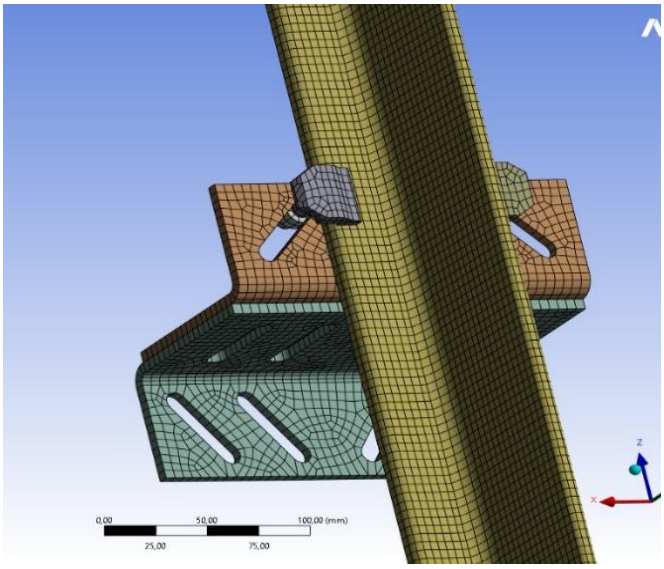

Fig. 7. Meshed system.

Since the guide rail's bottom surface is concreted to bottom of well, it is considered fixed end condition, that is, its rotations and translations are zero. Lower bracket surface overlaps with

the well wall and is fixed with a steel dowel so rotations and translations of this surface are considered to be zero. The elevator car applies Fx, Fy and Fk forces shown in Table 4 to the guide rail with shoes when safety device is activated during its vertical movement. Furthermore, a pre-tension force of 18000 N is applied to ensure the M8 bolt connections remain secure as depicted in Figure 8. The equivalent stresses and normal stresses occurred on investigated system were determined. TS EN 81 20 and TS EN 81 50 standards stipulate that allowable stress limit is 205 MPa when the safety device is activated. Allowable amount of bending deflection of guide rail with a safety device is 5 mm.

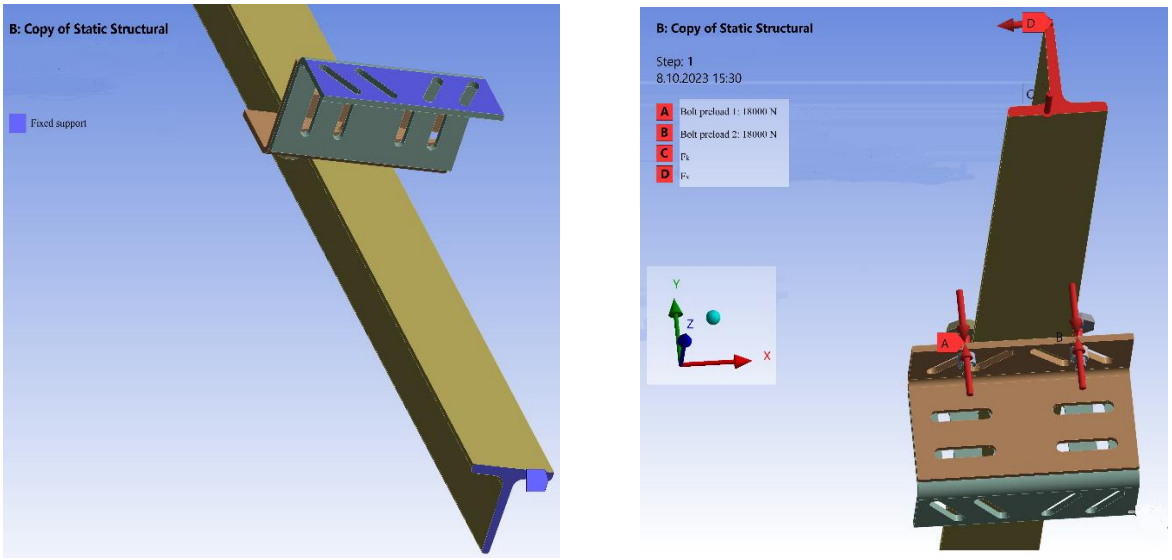

Fig. 8. Boundary conditions.

2.3. Experimental studies on guide rail bracket

Experimental measurements on elevator parts are arduous issue due to reasons such as finding new building to ready to install elevator assembly, obtaining permission to participate in full load tests during the elevator licensing process and the lack of mounting space yields hassle of connecting sensors to their places in elevator shaft.

Elevators are subjected to a full load braking test when obtaining a green label license. During this test, the cabin is charged homogeneously at 125% of its nominal load as shown in Figure 9. The loaded cabin is lifted to the top floor and initiated into free fall via the control panel. The motor driver detects the high speed and activate the safety gear with the regulator equipment. Meanwhile, the elevator locks itself to the guide rails and stops when the mechanical brake jaws attached to the cabin are activated.

Fig. 9. Homogeneous loading of the cabin with 1000kg weight.

The seventh bracket system for which experimental instrumentation will be performed is shown in Figure 10.

Fig. 10. Experimentally instrumented bracket system.

Spot normal stress value occurring on the upperside bracket was obtained for the situation in which the elevator's safety device was activated by means of strain gauge (SG) attached to the seventh bracket system. In this way, it is possible to compare the stresses determined in the experimental study with the stresses at the same point obtained in ANSYS finite element analysis (FEA). The strain gauge could not be attached to the certain point as it was impossible to mount it at the critical point where the normal stress determined on the bracket system by finite element analysis was maximum. For this reason, stress values determined in FEA at the node point 15813 indicated in Figure 16 could be compared with the normal stress value read from strain gage sensor connected to this point so node 15813 indicates the point where the strain gauge is attached to the bracket. Micro measurement SG sensors were used in the experimental study. For this type of SG sensor, there is no need for soldering after the bonding process is completed.

Measurements were made by means of NI cDAQ-9174 signal conditioner. Bracket surface to which C2A/06-250LW-350 type SGs are to be bonded has been prepared by means of tools and specified chemicals and then SGs were glued to bracket surface appropriate to strain gage user manual. Quarter bridge configuration in DaqExpress software was to acquire experimental data [27].

Signal conditioner circuit cables was taken into the elevator shaft through the shaft wall passing through a gap in the lower plate of the boarding door closest to the guide rail bracket to be measured. Experimental setup was prepared by means of SG's, wiring chasis, signal conditioner and laptop

Approximately 20 cm below the console system, the mechanical brake jaws squeezed the guide rail and the cabin stopped. Throughout the process, data were collected in terms of microstrain values (με) drawn from DAQExpress interface and the Figure 11 shows the damage caused by the safety device after the free falling test.

Fig. 11. Damage on the guide rail caused by the activation of the safety gear.

The SG glued elevator guide rail bracket before full load testing is shown in Figure 12.

Fig. 12. Instrumented guide rail bracket.

3. Results and discussion

In this study, a gearless passenger elevator that has already been installed in a building located in Zonguldak-Turkey province was examined. It consists of 7 stops with nominal load of 800 kg. and analytical calculations were made separately for the

cases that load distribution is located at the front (Figure 3a) and right (Figure 3b) and homogeneous load distribution (Figure 3c) within the cabin. The study examined a T 89/B type guide rail and an elevator car guided with a 70 mm eccentricity from the center. Mechanical stresses, deflections and forces exerted upon guide rail and its bracket taking into account different operating and loading combinations of investigated passenger elevator have been determined analytically where the safety gear is activated and presented in Table 4.

Table 4. Deflections, forces and stresses under different load distributions inside cabin.

Load distribution	F_x (N)	F_y (N)	F_k (N)	σ_x (N/mm^2)	σ_y (N/mm^2)	σ_{com} (N/mm^2)	δ_x (mm)	δ_y (mm)
Front	-1000.9	0	15696	0	39.76	49.76	2.07	0
Right	-541.08	797.1	15696	26.22	21.49	57.70	1.12	1.45
homogeneous	-584	0	17658	0	23.2	34.45	1.21	0

F_x force applied on guide rail changes since distances x_Q and x_P alter with different loading cases. In the load distribution at the right side, the presence of the distance y_Q as shown in Figure 3b caused the Fy force to be different from zero.

The reason why the buckling force is higher in homogeneous loading is that the nominal load is taken as 125% of nominal. The highest combined stress of 57.70 MPa was observed when the load distribution was applied on the right side.The reason is that the additional forces due to eccentricity of the controid of the empty cabin and the rated load on the y-axis increased the combined stress for right side loading condition. As the forces Fx and Fy vary, the rail neck bending also changes across different loading conditions. The maximum bending deflection of the rail neck, 2.07 mm in the x-direction, occurs under front loading distribution. The deflection, stress and force values exerted upon the T 89/B guide rail is found under permissible limits and safe. Equivalent stress changes on bracket system under different loading conditions where the safety device was activated were determined by finite element analysis.

The equivalent stress variation on guide rail bracket under front loading is depicted in Figure 13.

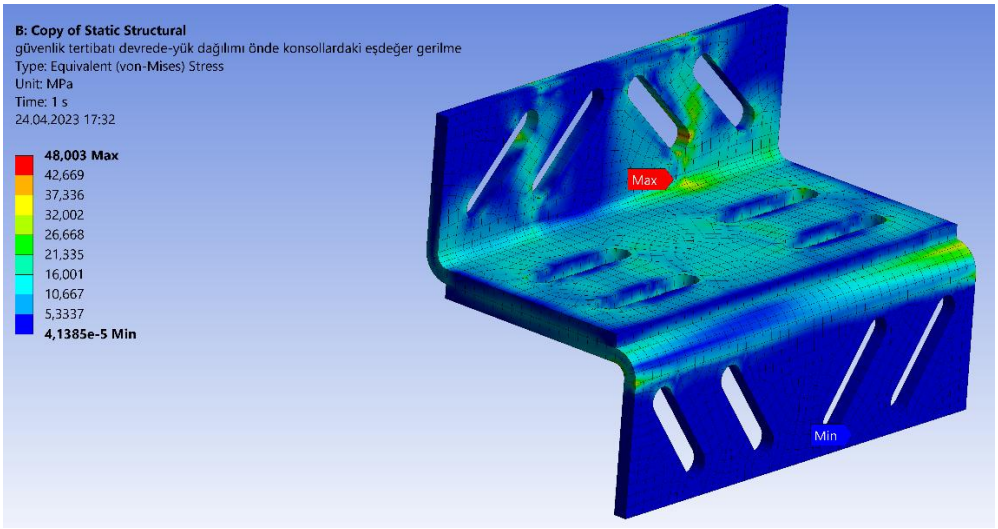

Fig. 13. Equivalent stress variation (front loading distribution).

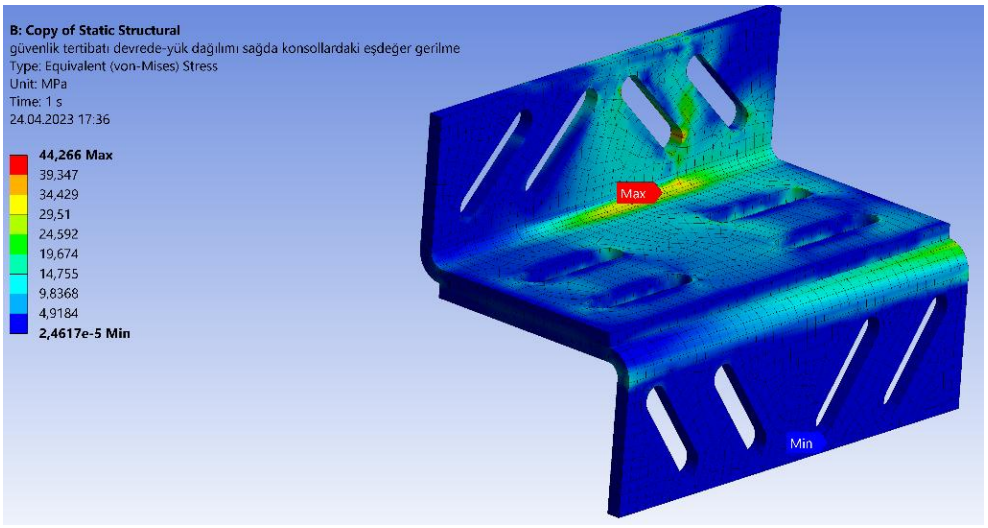

Fig. 14. Equivalent stress variation (Right loading distribution).

The equivalent stress variation on guide rail bracket under right loading is depicted in Figure 14.

The equivalent stress variation on the guide rail bracket under homogeneous loading is depicted in Figure 15.

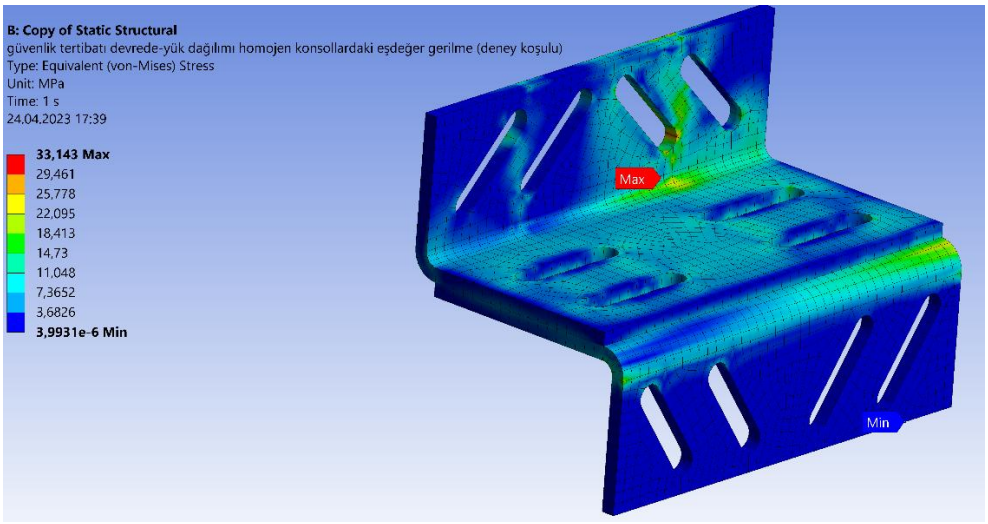

Fig. 15. Equivalent stress variation (Homogeneous loading distribution)

In the analyses, the forces carried by the guide rail were transferred to the upper bracket via nails, then to the lower bracket and finally to the well wall. Since the first contact occurs on the upper bracket, upper bracket is exposed to the maximum stress. Normal stresses also occur on the elevator system during running. FEA of the upper bracket component was carried out for normal stress distribution since maximum normal stress occurs in the upper bracket and SG sensors used in the experiments have been instrumented on upper bracket in case load distribution is homogeneous.

The normal stress variation on upper bracket under homogeneous loading is depicted in Figure 16.

When Figure 16 is examined, it is readily seen that the maximum normal stress measured by FEA at the bottom of the second housing hole from the right of the upper bracket is 27.578 MPa. Furthermore, the normal stress value at a location where the strain gauge will be attached on is found to be -7.0296 MPa. Figure 17 shows maximum equivalent stresses on bracket system measured by FEA for all loading distributions.

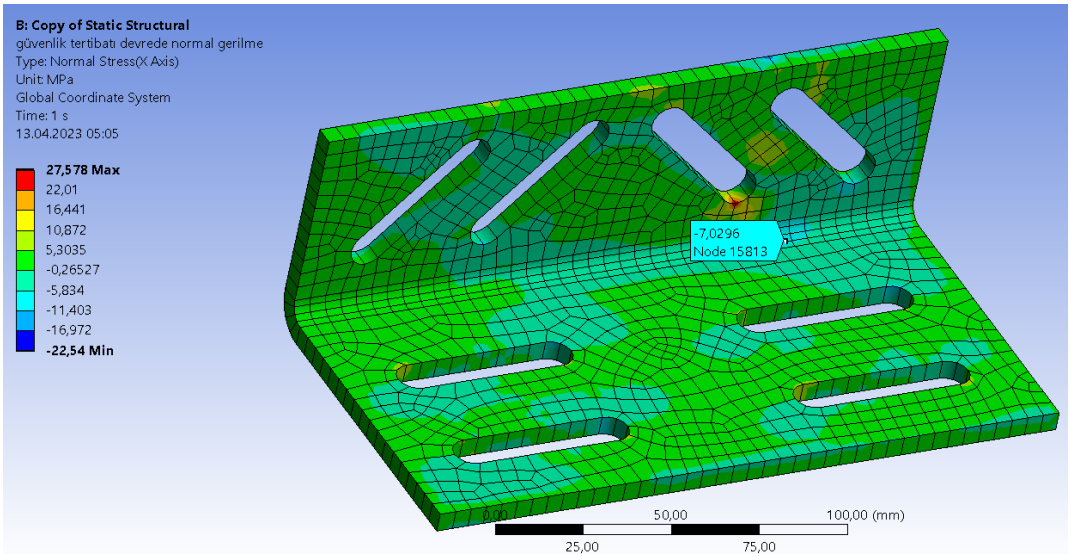

Fig. 16. Normal stress distribution under homogeneous loading.

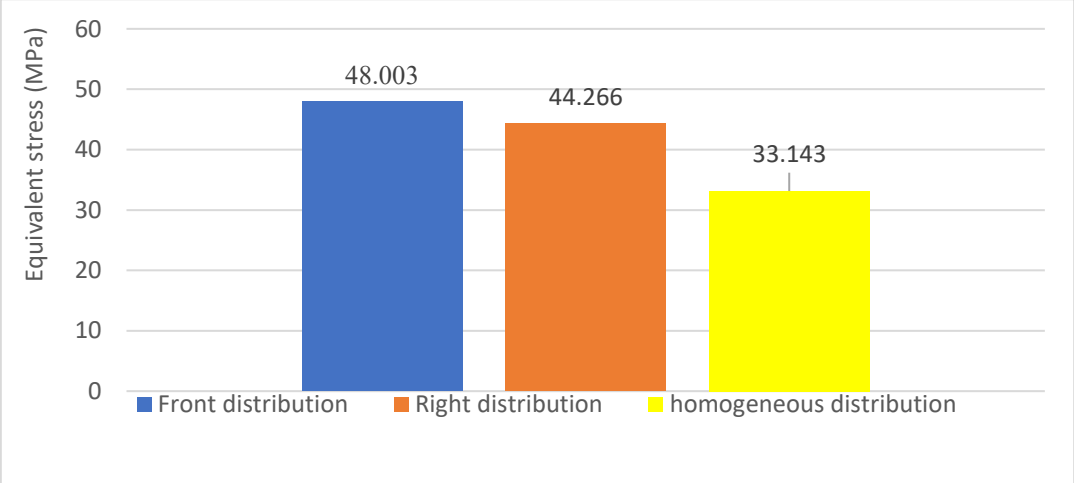

Fig. 17. Equivalent stress variations for all loading types.

When the results obtained from the finite element analysis were examined by considering the front, right and homogeneous loading conditions, the maximum equivalent stresses are measured to be 48.003 MPa, 44.266 MPa and 33.143 MPa respectively. The maximum equivalent stresses on bracket system are found by front loading condition. Results show that the most critical loading type for the bracket system occurs when three-fourths of the elevator cabin's load is distributed on the front side and equivalent stress was lowest in the homogeneous distribution. The reason why the guide rail brackets are subjected to greater stresses in front loading that the centroid moves farther away from the geometric center of the cabin and this distance is lowest at the homogeneous loading. Loading the elevator cabin from the front resulted in an 8.44% increase in maximum equivalent stress compared to right-side loading, and a 44.83% increase compared to uniformly distributed loading. The elevator system was evaluated under a full-load braking test. During test, loads were homogeneously distributed in the cabin at 125% of the nominal load. The cabin was lifted up to the top floor stop and forced to free fall from the control panel and safety gear was activated after motor driver detects the high speed. Since it was not possible to reach the point where maximum stress occurred, the strain gage was glued on the node point 15813 depicted in Figure 16. During the full-load braking test, strain data were recorded using DAQExpress and subsequently converted to stress values based on Hooke's Law. Figure 18 illustrates the experimental normal stress variations at the strain gauge location during the free fall and braking phases of the elevator cabin. Safety gear mechanics is activated by time interval 4-5 seconds and fully loaded elevator cabin is started to stop by means of locking of safety gear to the guide rails.

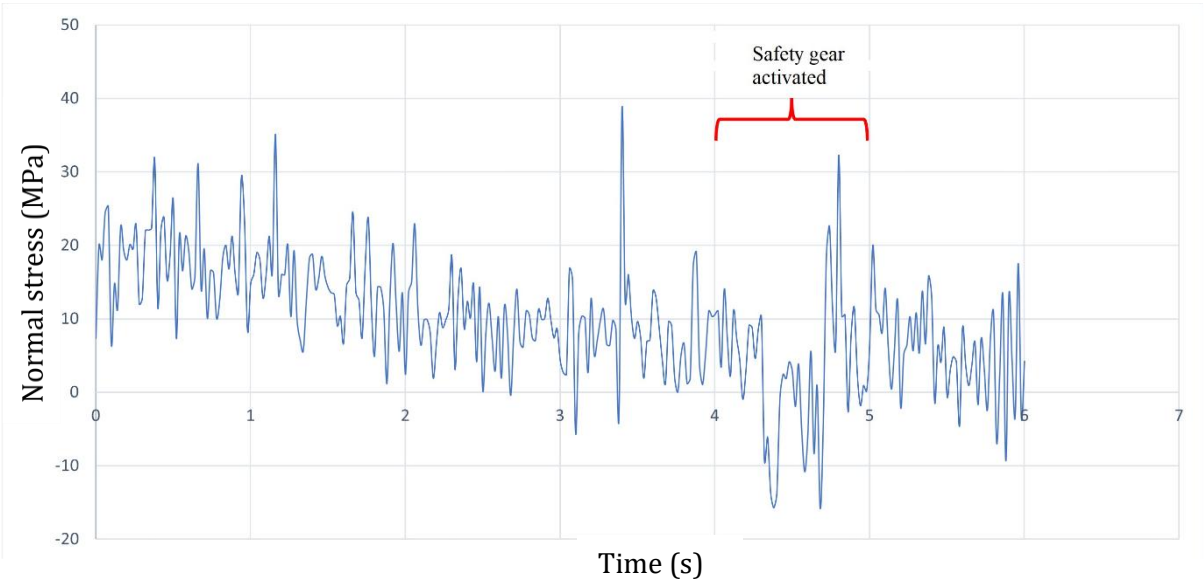

Fig. 18. Experimental stress variations on the bracket during free falling and braking.

The braking process took place between the 4.32 s - 4.70 s seconds after the test begun, and the arithmetic average of nine values taken from the signal conditioner was determined as -8.7596 MPa. The negative reading of the normal stress value is due to the fact that the strain gage mounting on the bracket is subjected to compressive stress on the ground. It can be seen from the Figure 18 that the pressure on the bracket is removed when the cabin completely stopped. Normal stresses on the upper bracket system, determined through experimental testing and numerical analysis, are shown in Figure 19.

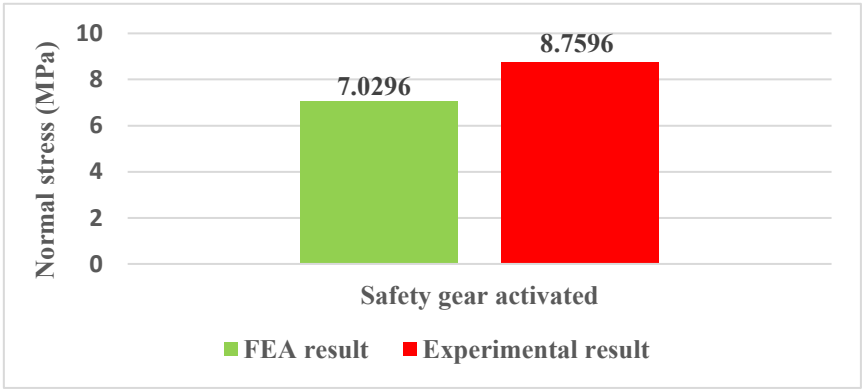

Fig. 19. Normal stresses on guide rail bracket.

Figure 19 illustrates the normal stresses on the upper bracket system measured experimentally and predicted numerically. The comparison shows that the experimental stress values are higher than those obtained from the finite element analysis (FEA) during elevator operation. The experimental results exhibit a 19.75% higher stress level compared to the FEA predictions. This discrepancy is likely due to the additional dynamic loading from sudden shocks during cabin movement and braking, which are not fully accounted for in the FEA model. It can be concluded from the findings that dynamic effects during the running and braking of the elevator have an effect of 20% compared to the results of the static analysis. In the near future, experimental studies are aimed at elevator installations with different guide rail support lengths, different floor numbers and different car capacities.

4. Conclusions

In this study, a gearless passenger elevator that has already been installed in a building located in Zonguldak-Turkey province was examined. Analytical, numerical and experimental calculation, instrumentation and measurements were made considering international norms for elevator guide rail and its brackets where the safety gear is activated. Under front loading distribution, the rail neck experiences a maximum bending deflection of 2.07 mm in the x-direction. The bracket system experiences the highest equivalent stresses when three-fourths

of the elevator cabin load is applied at the front, making this the most critical loading condition. Under front loading, the maximum equivalent stress rises by 8.44% compared to right-side loading and by 44.83% compared to a homogeneous load distribution. The maximum normal stress measured by FEA at the bottom of the second housing hole from the right of the upper bracket is 27.578 MPa. Elevator investigated was subjected to a full load braking test. During test, the cabin is charged homogeneously at 125% of its nominal load. Normal stress variation during braking process were measured by using strain gages and arithmetic average of measured values was found by using signal conditioner. Normal stress was determined as -8.7596 MPa on point where strain gage was connected where normal stress value was found as -7.0296 MPa by FEA. It can be concluded from the findings that dynamic effects during the running and braking of the elevator have an effect of nearly 20% compared to the results of the static analysis.

Acknowledgements

This study was supported by Zonguldak Bulent Ecevit University Scientific Research Fund (Project No. 2021-77654622-11).

References

1. Strakosch G R. The vertical trasportation handbook. 3rd ed. Canada: Wiley: 1998. https://doi.org/10.1002/9780470172865
2. İmrak C E, Gerdemeli İ. Elevators and escalators. 1st ed. Turkey: Birsen: 2000.
3. Koc S, Imrak C E, Targit S. Design parameters and stress analysis of elevator guide rail brackets, Elevator World. 2011, 6: 96-103.
4. Atay S, Salman O, Imrak C E. Experimental studies on guide rail fastening system, The 5th symposium on lift and escalator technologies, Northampton, UK, 23-24 September 2015: 21-28.
5. Xu P, Peng Q, Jin F, Xue J, Yuan H. Theoretical and experimental study on tension–torsion coupling vibration for time-varying elevator traction system. Acta Mech Solida Sin. 2023, 36: 899–913. https://doi.org/10.1007/s10338-023-00429-5.
6. Ma X, Pan G, Zhang P, Xu Q, Shi X, Xiao Z, Han Y. Experimental evaluation of braking pad materials used for high-speed elevator, Wear. 2021, 477: 203872. https://doi.org/10.1016/j.wear.2021.203872.
7. Janovsky L. Elevator mechanical design, 3th ed. USA: Elevator World: 1999.
8. Wu A, Shi X, Weng L, Hu D. Thermo-mechanical modeling and transient analysis of frictional braking of elevator safety gear. J Therm Stresses. 2020, 43:1467-86. https://doi.org/10.1080/01495739.2020.1820921.
9. Shuka H, Al-Wajidi W. Stress analysis of guide rails of elevators. Khwarizmi Eng J. 2009, 5: 38-50.
10. Altuntas M, Salman O, Imrak C E. Experimental stress analysis of elevator guiding equipment. Key Eng Mater. 2017, 572: 177-80. https://doi.org/10.4028/www.scientific.net/KEM.572.177.
11. Ozek C, Suer E. Analysis of stress distribution occurring in guide rails for different positions of elevator car by finite element method. Fırat University Journal of Engineering Science. 2023, 35: 923-935. https://doi.org/10.35234/fumbd.1272957.
12. Benli O H, Selek M, Ergen B, Yıldız O. The Effects of short braking distance on car sling construction in L type elevator systems. Trakya Univ J Eng Sci. 2023, 24: 19-28. https://doi.org/10.59314/tujes.1279083.
13. Han Q, Zhang X, Lu Y, Wang L. Experimental investigation on the in-plane mechanical behavior of elevator guidance system. J Build Eng. 2023, 76:107333. https://doi.org/10.1016/j.jobe.2023.107333.
14. Goluch P, Kuchmister Cmielewski J K, Brys H. Multi-sensors measuring system for geodetic monitoring of elevator guide rails. Measurement. 2018, 130: 18-31. https://doi.org/10.1016/j.measurement.2018.07.077.
15. Zhang J, Lu H, Jiang H, Miao Y, Shi Z, Study on reliability of emergency braking performance of high-speed and heavy-load monorail crane. Eksploatacja i Niezawodnosc – Maintenance and Reliability. 2024, 26(1): 1-17. http://doi.org/10.17531/ein/174820.
16. Zheng Q, Wang D, Zhang K, Ma J, Ding G, Zhang Y, Yuan Z. A parametric study on the fatigue life of elevator brake wheels under multi-field coupling effects. Eng. Fail. Anal. 2025, 167: 1-17. http://doi.org/10.1016/j.engfailanal.2024.109061.
17. Zhang J, Liu M, Li M, Liu B, Jin S, Qin L, Ma J, Zhang H, Xu L. Simulation and experimental study on the aerodynamic characteristics of a high-speed elevator with three-sided arc fairings. J Build Eng. 2024, 81: 108172. http://doi.org/10.1016/j.jobe.2023.108172.
18. Niu D, Guo L, Zhao W, Li H. Operation performance evaluation of elevators based on condition monitoring and combination weighting method. Meas. 2022, 194: 111091. http://doi.org/10.1016/j.measurement.2022.111091

19. Lee D S, Ji K H, Jing J, Jo J H. Experimental study on elevator door reopening problems caused by stack induced pressure differences across the elevator door in buildings. Build. Environ. 2022, 221: 109271. http://doi.org/10.1016/j.buildenv.2022.109271.
20. Zhang S, Zhang Q, Su X, Zhao Z, He Q, Meng L. Research on explicit model predictive control method for horizontal vibration of high-speed elevator car system. *J. Braz. Soc. Mech. Sci. Eng. 2025,* 47: 42. http://doi.org/10.1007/s40430-024-05349-0.
21. TS EN 81-20. Safety rules for the construction and installation of lifts - Lifts for the transport of persons and goods - Part 20: Passenger and goods passenger lifts. Ankara: Turkish Standards: 2020.
22. TS EN 81-50, Safety rules for the construction and installation of lifts - Examinations and tests - Part 50: Design rules, calculations, examinations and tests of lift components. Ankara: Turkish Standards: 2020.
23. Koç S. Elevator guide rail brackets stress analysis, Istanbul Technical University, Graduate School of Science and Engineering, MSc Thesis, İstanbul: 2009.
24. Mert Ö, Yeter İ, Tavaslıoğlu S. Stresses occurring in elevator consoles and connection parts. Elevator symposium, İzmir, Turkey, 18-20 September 2018: 1-19.
25. TMMOB, Technical Principles for Preparing Elevator Preliminary and Implementation Projects. 7th ed. İzmir: Chamber of Mechanical Engineers Publications: 2012.
26. Onur Y A. Finite element modeling of elevator carframes and stress analysis, İstanbul Technical University, Institute of Science and Technology, MSc thesis, İstanbul: 2006.
27. Onur Y A. Experimental and theoretical investigation of prestressing steel strand subjected to tensile load. Int J Mech Sci. 2016, 118: 91-100.https://doi.org/10.1016/j.ijmecsci.2016.09.006.